QUANTIFICATION FOR THE ENERGY FACTOR OF DAMAGE-CONTROL TCBSBFS SUBJECTED TO NEAR-FAULT SEISMIC RECORDS

R. Zhang[(1)], W. Wang[(2)]

[(1)] *PhD candidate, State Key Laboratory of Disaster Reduction in Civil Engineering, Tongji University, Shanghai 200092, China, zhangruibin@tongji.edu.cn*
[(2)] *Professor, State Key Laboratory of Disaster Reduction in Civil Engineering, Tongji University, Shanghai 200092, China, weiwang@tongji.edu.cn*

Abstract

The tension-only concentrically braced steel beam-through frames (TCBSBFs) are compelling options for low-to-medium rise buildings in low to moderate seismic regions. The TCBSBFs can demonstrate the damage-control behaviour with inelastic damages limited to braces for a wide deformation range, and concurrently the post-earthquake residual displacement was minimised. This paper quantifies the seismic demand of damage-control TCBSBFs under pulse-like near-fault earthquake motions. Firstly, the hysteretic model of TCBSBFs in the damage-control stage is validated based on the test database of a prototype structure. Subsequently, representative single-degree-of-freedom (SDOF) systems with the verified hysteretic law are subjected to 320 pulse-like near-fault seismic records. A parametric study including more than 8,208,000 nonlinear spectral analyses is carried out. The effect of the hysteretic parameters (i.e. the post-yield stiffness ratio and the ductility in the damage-control stage) and the damping ratio on the energy factor is examined in detail. The results revealed that the energy factor demand of bilinear slip kinematic SDOF systems representing the TCBSBFs under pulse-like near-fault earthquakes is sensitive to the hysteretic parameters in the damage-control stage. An increasing post-yield stiffness ratio (α) leads to a decreasing energy factor (γ) in the short and moderate period regions, while the tendency is reversed for the long period region. In contrast, a larger ductility (μ) leads to a higher γ in the short and moderate period regions, whereas the tendency is also reversed for the long period region. For the effect of the damping ratio (ζ), a larger ζ leads to an increase of γ while the reversed tendency can be observed when both α and μ are extremely high. The influence of α and μ on γ is more obvious in the short and moderate period regions than in the long period region. Besides, μ has limited influence on the γ in the long period region in the case with a significant α. On the basis of 8,208,000 computed values of the energy factor, the probabilistic distribution of the energy factor exhibits certain degree of positive skewness. In order to ensure the seismic reliability of TCBSBFs, a probabilistic model of the seismic energy factor governed by the lognormal distribution is developed to facilitate the performance-based seismic design of TCBSBFs. Based on regression analysis of the database, two empirical formulas are proposed for two key parameters. The design model may offer practical guidelines for design of the TCBSBFs. Finally, the design-check process of a three-story tension-only concentrically braced steel beam-through frame is illustrated using the spectral model of γ.

Keywords: Beam-through frame, Tension-only braces, Energy factor, Probabilistic model

1. Introduction

The tension-only concentrically braced steel beam-through frame (TCBSBF) is a novel system composed of I/H-section “through beams”, cold-formed square-tube columns and slender X-braces fabricated by flat steel [1-5]. The through beams and columns contribute towards the “primary frame”, whilst the braces may resist lateral loads. In engineering practices, all components of TCBSBFs can be prefabricated in factory and assembled through high-strength bolts in construction sites, which enables rapid construction, making the structural system economical and sustainable.

In this context, it is desirable to explicitly account for damage-control behaviour of TCBSBFs, which contributes to avoiding the soft-storey failure mechanism directly. Recent studies show that an energy factor [6] uniting the strength demand and deformation demand is a compelling demand indicator for seismic design and evaluation of the structure [7-12]. Concurrently, the probabilistic seismic demand model of the structure is of growing importance in modern seismic engineering, because it may offer sufficient flexibility for designers and decision makers to choose an expected limit space [13]. Hence, quantifying the seismic demand and developing a probabilistic seismic demand model for TCBSBFs are desirable to guarantee the seismic safety of the novel systems in both design and evaluation procedures.

In this study, based on a classical bilinear slip model validated by test results, the nonlinear behaviour of the TCBSBFs deforming in the damage-control stage is reviewed and quantified. Subsequently, the energy factor of single-degree-of-freedom (SDOF) systems assigned with the verified hysteretic model is analysed using 320 pulse-like near-fault seismic records as input excitations. The effect of the hysteretic parameters and the damping ratio on the energy factor is examined in detail. Based on the obtained data, it is proved that the lognormal distribution model could well describe the probabilistic distribution of the energy factor. Finally, in order to easily apply in practical design and evaluation procedures, two empirical formulas are fitted for the key parameters in the lognormal distribution model of the energy factor. A three-story tension-only concentrically braced steel beam-through frame is designed based on the spectral model of γ.

2. Review of the hysteretic behaviour and dynamic response of the structure

2.1 Review of the experimental works

Recently, full-scale experimental studies [1, 2] (i.e. quasi-static and shake table tests) of TCBSBFs have been conducted to provide an insight into the hysteretic behaviour and dynamic response of the structure under earthquakes. Figs. 1(a) and 1(b) reproduce the test arrangement of full-scale quasi-static and shake table tests structures, respectively. More details about the test programme can be found in [1].

(a) (b)

Fig. 1 – The previous tests of full-scale TCBSBFs: (a) Quasi-static test [1] (b) Shake table test [2]

2.2 Hysteretic model and verification

The typical hysteretic response of the TCBSBFs extracted from the previous test database [1, 2] is reproduced in Fig. 2(a). As shown in Fig. 2(a), the hysteretic behaviour can be divided into two stages: (1) In the damage-control stage (DCS), the primary frame remains elastic except for the tension-only braces which are easy to replace. Moreover, there is no significant residual displacement. (2) In the ultimate stage (US), beam-column connections progress into plasticity, and hence the residual displacement increases significantly. Note that the analysis of seismic behaviour and demands of TCBSBFs in damage-control stage will be focused on in this paper, and the ultimate stage is not within the scope of the current study.

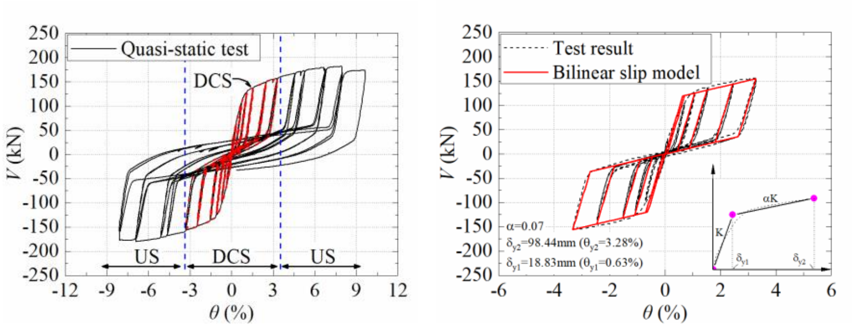

(a) (b)

Fig. 2 – Hysteretic model and verification: (a) The typical hysteretic response of the TCBSBFs (b) Comparison of test result and the bilinear slip model.

According to the test results, it can be confirmed that the hysteretic response of the structure deforming in the damage-control stage follows the classical bilinear slip kinematic hysteretic law. As shown in Fig. 2(b), the adequacy of the bilinear slip hysteretic model for replicating the hysteresis of TCBSBFs in the damage-control stage was validated by comparing the bilinear slip model curve with the test responses.

3. Energy factor of oscillators representing TCBSBFs

3.1 Definition of the energy factor and implications

Housner [14] firstly proposed the energy balance design concept for elasto-perfectly plastic (EP) system in the last century. In a design context, the area under skeleton load-deformation curve of the elastic system is approximately equal to that of inelastic system, which is known as the “equal-energy rule”. Later, Newmark and Hall [15] found that the “equal-energy rule” is valid only for a certain period range. Recently, Lee and Goel [16] proposed the energy factor (γ) to modify the energy balance equation in such a way that the design concept of energy balance can be applied to all period ranges.

According to the illustration of the energy balance in Fig. 3, the energy factor is obtained and given by [17]

$$\gamma = \frac{E_a}{E_{ae}} = \frac{\left[2\mu - 1 + \alpha\left(\mu - 1\right)^2\right]}{R^2} \tag{1}$$

where R is the strength reduction factor, Ea is the nominal energy capacity of the structure and Eae is the absorbed energy of the corresponding elastic system.

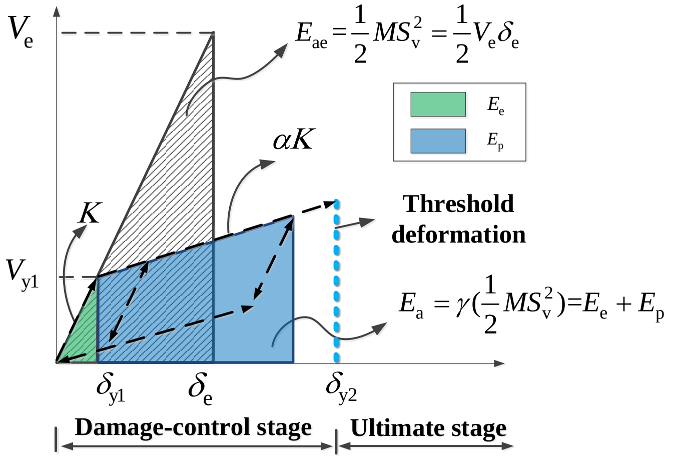

Fig. 3 – Energy factor of a bilinear slip SDOF system with presence of the DCS.

3.2 Ground motion database

Pulse-like near-fault ground motions exhibiting two important characteristics, a pulse-like velocity waveform and a permanent ground displacement, which generally induce large seismic demand [18]. Therefore, it is of great interest to study the energy factor of TCBSBFs subjected to such earthquake motions. In the present study, a large ground motion database has been compiled. The near-fault ground motions samples have also been used in works of Hatzigeorgiou [19] or Dabaghi [20]. The ground motion database constitutes 320 near-fault pulse-like ground motions with a magnitude range of 5.5-7.9 from a variety of active tectonic regions (i.e. strike-slip, reverse, oblique and normal fault types). These records are recorded at sites where the closest distance to the fault rupture is less than or equal to 30.5 km.

3.3 Parameter matrix

A comprehensive parametric study is conducted to examine the effect of the hysteretic parameters (i.e. the post-yield stiffness ratio and the ductility in the damage-control stage) and the damping ratio on the energy factor of oscillators representing the TCBSBFs in the damage-control stage. In order to examine the influence of α on the energy factor of this system, fifteen values of α are set for oscillator varying from 0 to 0.7 with an increment of 0.05 in the present work. The ductility (μ) of the TCBSBFs in the damage-control stage varies from 1.5 to 6.0 with an increment of 0.5 (i.e. ten values of μ) to investigate the effect of μ on the energy factor. The damping ratio (ζ) is increased from 1% to 5% with an increment of 2% assumed in the analyses. Fifty-seven (57) vibrating periods varying from 0.2 s to 3.0 s with an increment of 0.05 s are included in the parameter matrix. Thus, a total number of 15 × 10 × 3 × 57 × 320 = 8,208,000 energy factor values are calculated.

4. Analytical results and discussions

4.1 Effect of the hysteretic parameters and damping ratio on energy factor

As given in Figs. 4, 5 and 6, representative mean γ demand spectra are utilised to demonstrate the influence of the post-yield stiffness ratio (α), the ductility (μ) and the damping ratio (ζ) on the energy factor (γ) of the TCBSBFs in the damage-control stage. A reference case is selected with a constant damping ratio of 5% to explain the influence of α and μ on γ. As shown in Figs. 4 and 5, the curves intersect at certain period defined as the characteristic period Tr, which generally varies from 0.5 to 1.1s.

To illustrate the effect of α on the energy factor demand of TCBSBFs under pulse-like near-fault records, three representative figures of mean γ demand spectra corresponding to fixed μ and varying α are presented in Fig. 4. Generally, the energy factor (γ) notably reduces when α increases in the region T < Tr, whereas the tendency is reversed in the region T ≥ Tr. It is shown in Fig. 4(c) that this trend is more remarkable for systems with larger μ by comparison with Fig. 4(a). This suggests that it is more efficient to increase α to reduce the seismic demand of the structure with high ductility when the period of structure is less than the characteristic period. In Fig. 5, three representative figures with the same α and different μ highlight the influence of μ on γ. The results in Fig. 5 imply that a higher μ results in a larger γ in the region T < Tr, while the tendency is reversed for the region T ≥ Tr. This phenomenon is more evident for systems with smaller α. It is of interest to find that compared with the tendency in the region T < Tr, the μ has limited influence on γ in the region T ≥ Tr, especially when α is significant. Besides, it is observed that a larger α pushes the characteristic period Tr shifting toward to the right side (i.e. a larger value of Tr). For the effect of the damping ratio (ζ), a larger ζ generally leads to an increasing of γ as shown in Fig. 6(a) and Fig. 6(b). However, results in Fig. 6(c) unveil that the reversed tendency can be observed when both α and μ are extremely high.

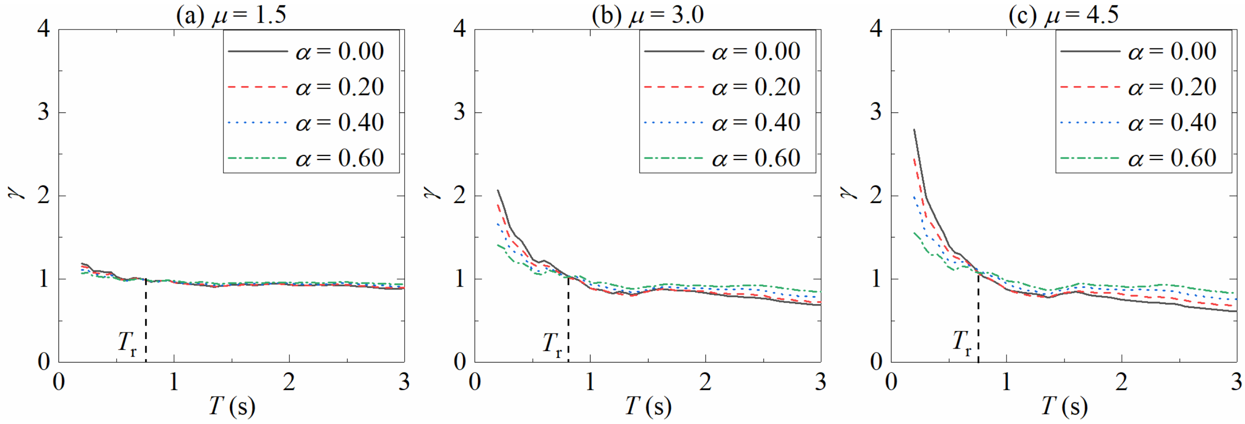

Fig. 4 – Effect of the post-yielding stiffness ratio (α) (ζ = 5%).

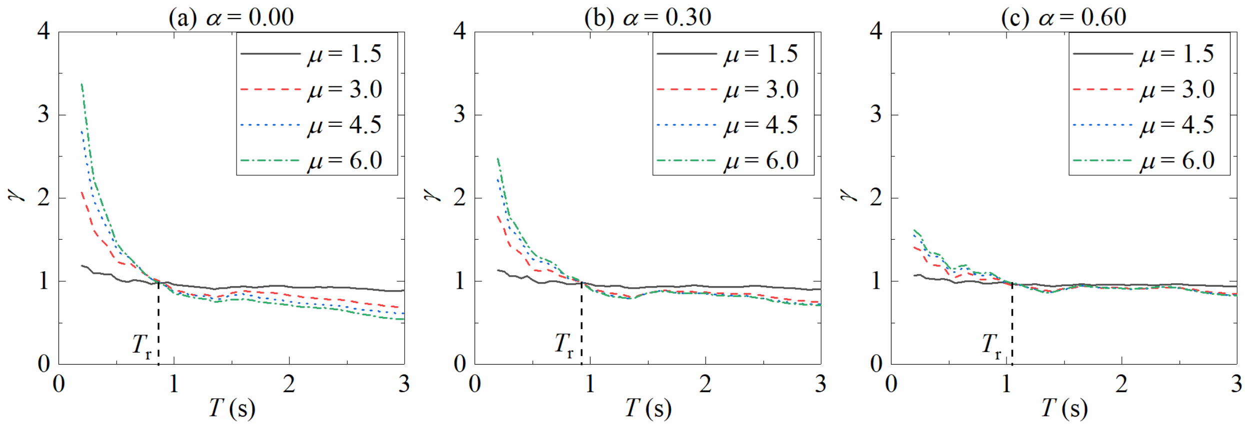

Fig. 5 – Effect of the ductility (μ) (ζ = 5%).

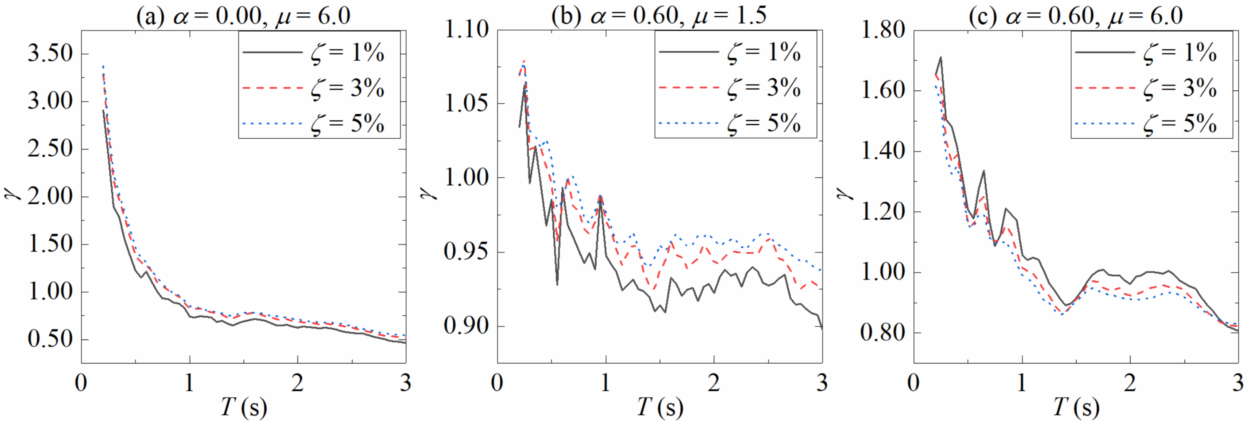

Fig. 6 – Effect of the damping ratio (ζ).

4.2 Effect of the hysteretic parameters on dispersion of energy factor

To clarify the dispersion of the energy factor, the heat maps of the probability of γ are obtained. For an equivalent SDOF system with predetermined α and μ, 57 probability histograms can be computed under 57 vibrating periods (i.e. from 0.2 s to 3 s with an increment of 0.05 s). Plotting all the results into one figure, a heat map of the probability of γ can be obtained with predetermined α and μ. Considering fifteen (15) α values and ten (10) μ values under 5% damping ratio, 150 heat maps of the probability of γ will be calculated. For brevity, six representative heat maps of the probability of γ under different α and μ are given in Figs. 7 and 8. In Fig. 7, the results show that the enhancement of α can lead to reduction of the deviation of γ. For the effect of μ on the dispersion of the energy factor, it is confirmed that the deviation of γ could be significantly reduced when μ decrease as shown in Fig. 8. In general, the dispersion of γ is higher in the region T < Tr than that in the region T ≥ Tr. The phenomenon is more evident when α is smaller or μ is higher, according to Fig. 7(a) and Fig. 8(c).

Notably, the probabilistic distribution of γ exhibits certain degree of positive skewness corresponding to a predefined T, α and μ. Besides, the skewness of distribution of γ differs from each other with different T values. In case with a small α or a high μ, the skewness is more obvious in the region T ≥ Tr as shown in Fig. 7(a) and Fig. 8(c). Nonetheless, the skewness is not evident when T is extremely small in this case. As the lognormal distribution is one of the most commonly used probabilistic distribution to quantify the positively skewed statistic distribution, a probabilistic model of γ will be developed in the following section in order to describe the statistic distribution of the energy factor demand.

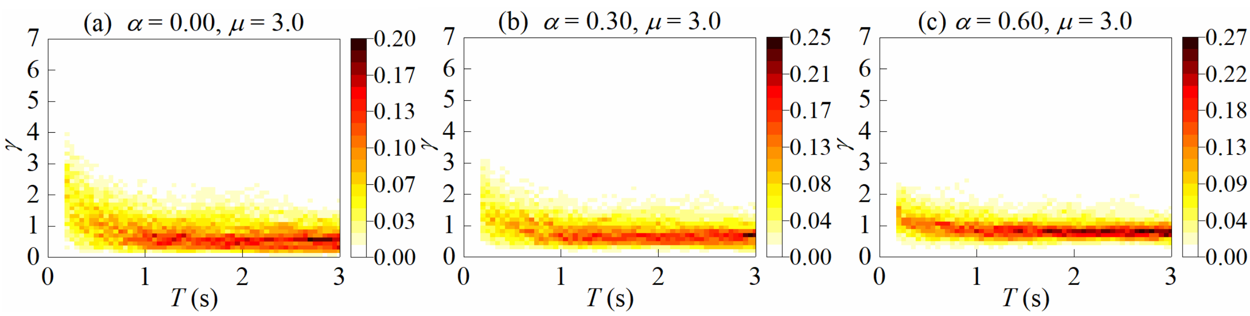

Fig. 7 – Effect of α on the statistic property of γ (ζ = 5%).

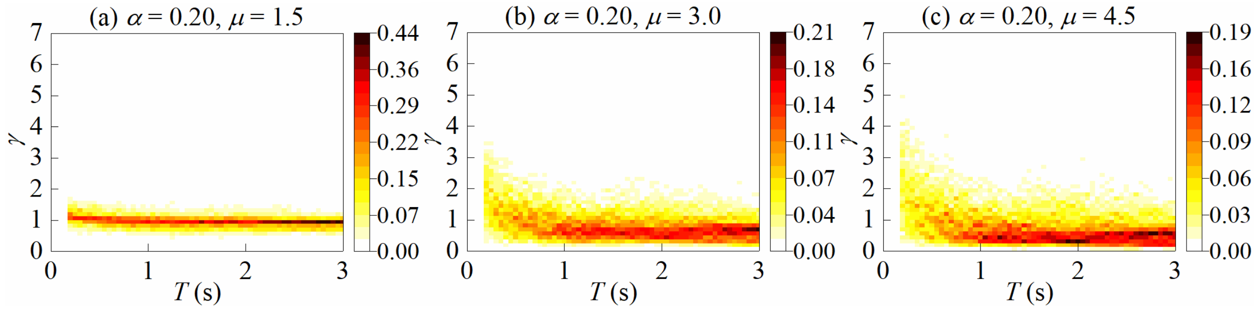

Fig. 8 – Effect of μ on the statistic property of γ (ζ = 5%).

5. Design considerations

5.1 Probabilistic model of the energy factor for TCBSBFs

The probabilistic seismic demand model is promising for the design of structures to choose a proper limit by taking into account the importance of the structure and economic aspects. Thus, the probabilistic properties of the seismic demand of γ based on the lognormal distribution will be explored in this section.

For a predetermined α and μ, the histogram of γ is plotted under given T to illustrate the probabilistic properties of γ. The probabilistic density function (PDF) of lognormal distribution for γ could be represented as

$$\mathrm{PDF}(x) = \frac{1}{x} \cdot \frac{1}{\sqrt{2\pi}\,(\ln\gamma)_{\mathrm{s.dev}}} \cdot \exp\left\{ -\frac{\left[\ln x - (\ln\gamma)_{\mathrm{ave}}\right]^2}{2\left[(\ln\gamma)_{\mathrm{s.dev}}\right]^2} \right\} \tag{2}$$

where x is a certain possible value of γ for seismic design; lnγ is the natural logarithm of γ; (lnγ)ave and (lnγ)s.dev are the mean and standard deviation of lnγ, respectively. Then the comparison between the histogram of γ and its PDF curve given by Eq. (2) is conducted to examine the adequacy of the lognormal distribution model for quantifying the probabilistic properties of γ. As similar trend is observed after the comparisons are tested for all combinations of α, μ and T, three representative results corresponding to α = 0.2, μ = 3.0 and ζ = 5% are listed in Fig. 9. It can be seen that the lognormal distribution of Eq. (2) is a proper description in describing the probabilistic distribution of γ.

Fig. 10 gives the Quantile-Quantile plots of the computed γ distribution versus their lognormal simulation corresponding to the nine figures in Fig. 9. As shown in Fig. 10, the lognormal distribution fitted in Fig. 9 could provide a good estimation of the probabilistic distribution for the energy factor demand of TCBSBFs under pulse-like near-fault earthquake motions. Nonetheless, the lognormal distribution may lead to compromised estimation of the energy factor demand in the extremely short period region.

In essence, (lnγ)ave and (lnγ)s.dev in Eq. (2) are two key parameters to determine the lognormal distribution model of γ. Besides, these two parameters are influenced by the value of T under each pair of α and μ. In order to make structural design and evaluation procedures more convenient, the empirical expressions of (lnγ)ave and (lnγ)s.dev are developed in the current work.

The empirical expressions of (lnγ)ave are fitted by the equation

$$(\ln\gamma)_{\mathrm{ave}} = AT^B + C \tag{3}$$

where A, B and C are fitting coefficients that relate to different pairs of α and μ. Similarly, the empirical expressions of (lnγ)s.dev are fitted by equation

$$(\ln\gamma)_{\text{s.dev}} = DT^2 + ET + F \tag{4}$$

where D, E and F are fitting coefficients also relating to different pairs of α and μ. The representative fitted curves are presented in Figs. 11 and 12.

Then, the cumulative distribution function (CDF) of γ could be computed as the following equation

$$\text{CDF}(x) = \Phi\left[\frac{\ln x - (\ln\gamma)_{\text{ave}}}{(\ln\gamma)_{\text{s.dev}}}\right] = \Phi\left[\frac{\ln x - \left(AT^B + C\right)}{DT^2 + ET + F}\right] \tag{5}$$

where x is the threshold of seismic demand under certain performance level; Φ represents the standard normal distribution.

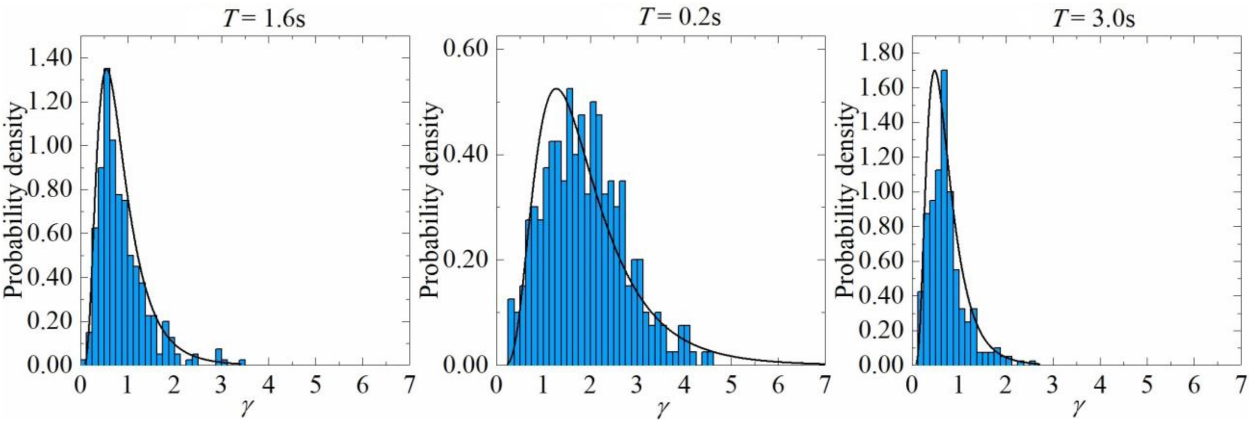

Fig. 9 – Histogram vs. PDF curves of γ distribution under different T (α = 0.2, μ = 3.0, ζ = 5%).

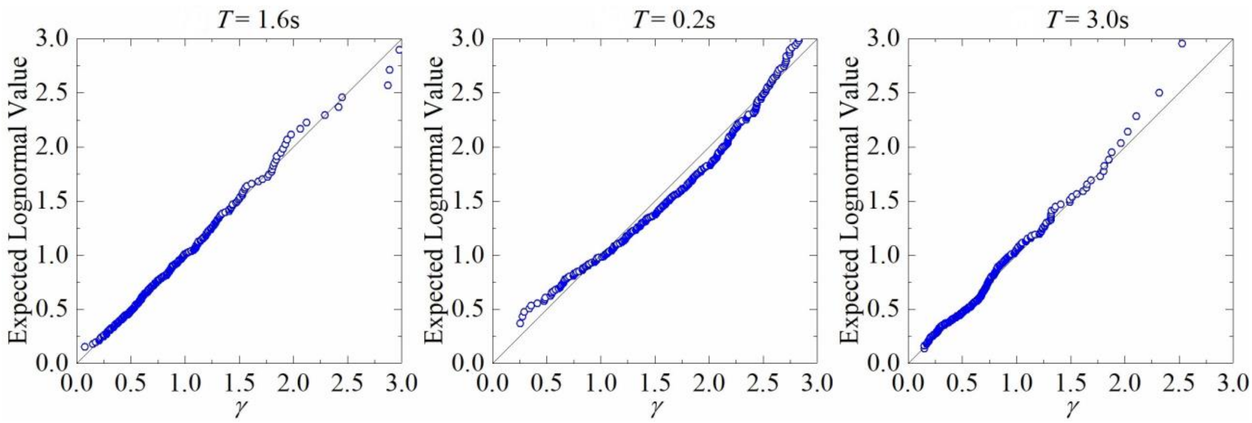

Fig. 10 – Quantile-Quantile plot of γ distribution fitted by lognormal distribution (α = 0.2, μ = 3.0).

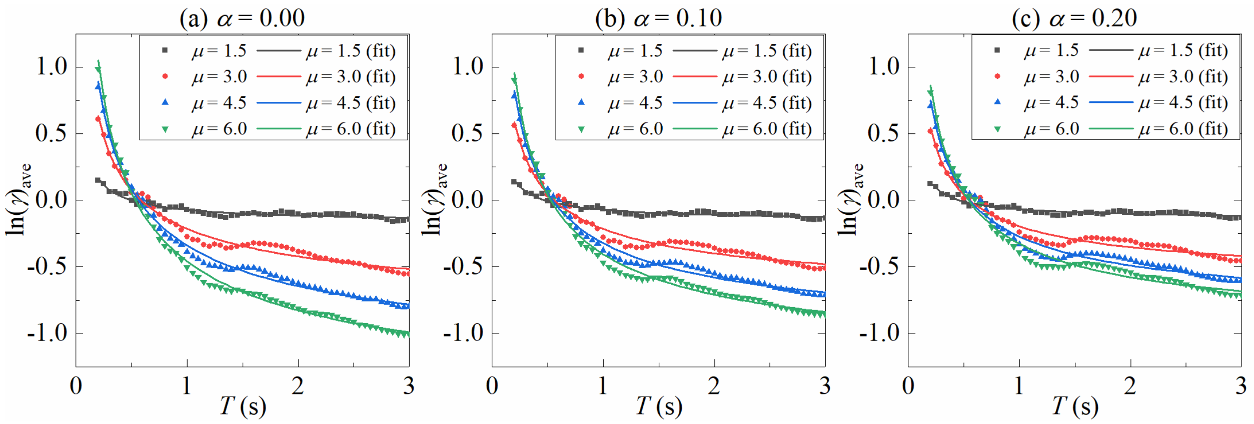

Fig. 11 – The (lnγ)ave-T points and the fitted (lnγ)ave-T curves.

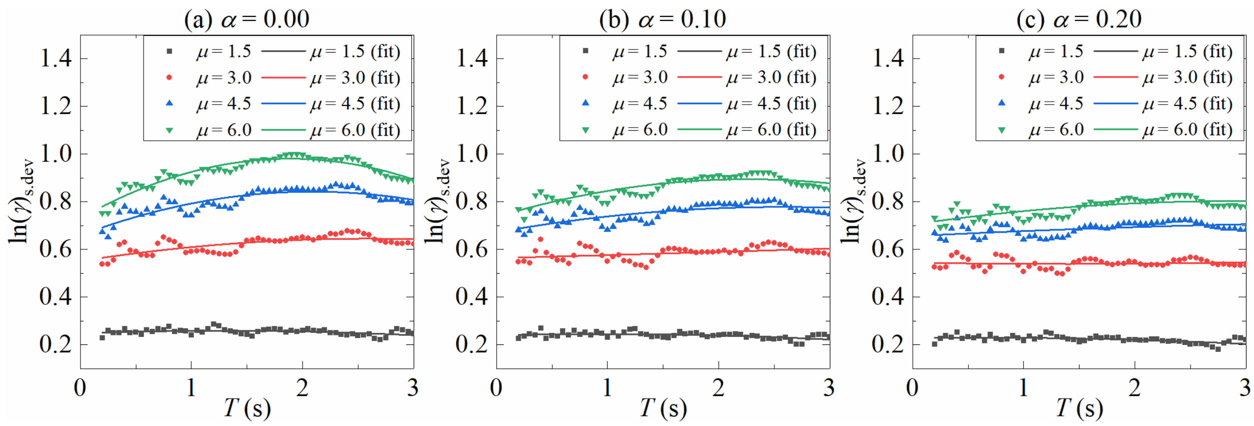

Fig. 12 – The (lnγ)s.dev-T points and the fitted (lnγ)s.dev-T curves.

5.2 Further design comments

The results obtained above are practical to guide an engineer to design TCBSBFs. Specifically, for the effect of the post-yield stiffness ratio (α), when the fundamental period (T) is in the short and moderate period regions, it is recommended to enhance α to reduce the energy factor (γ) with a given target ductility (μ). The reduction of γ is beneficial to achieve the design objective. However, when T of a structure is in the long period region, the reduction of α is recommended with a given target μ. As for the effect of the ductility (μ), it is expected to have a lower target μ when T of a structure is in the short and moderate period regions with a given α. In contrast, a higher target μ is favourable when T of a structure is in the long period region.

The results from Figs. 7 and 8 imply that a larger α and a smaller μ are favourable to reduce the dispersion of γ, eliminating the response uncertainty of a TCBSBFs under seismic events. In practice, designers may optimise the design by adjusting the hysteretic parameters of TCBSBFs.

In summary, when designing or evaluating the damage-control behaviour of a low-to-medium rise TCBSBFs governed by the fundamental vibration mode, the essential hysteretic parameters (i.e. α and μ) of the damage-control stage can be determined using a fundamental-mode-based pushover analysis as a start point. Then, the nominal energy demand can be calculated based on the CDF of γ demand according to the design objective and earthquake motion characteristics. Concurrently, the energy capacity till the damage-control threshold can be determined using the pushover database. In particular, the nominal energy capacity may be computed based on the work done by the lateral pushover loads according to the work-energy principle. Therefore, a damage-control index is developed and given as follows:

$$D = \frac{\frac{WgT^2}{8\pi^2}\gamma(\alpha,\mu,\zeta)S_a^2}{E_a(\mu)} \tag{6}$$

where Sa is the spectral acceleration that corresponds to the fundamental period of the structure; W is the seismic weight of the entire structure; g is the gravitational acceleration; T is the fundamental period of the structure.

In cases where the index is lower than unity, indicating that the nominal energy capacity is higher than the corresponding demand before the structure progresses into the post-damage-control stage, the system could achieve the damage-control behaviour by limiting inelastic actions in the braces. Otherwise, the structure is expected to deform into the ultimate stage. Thus, the CDF of γ demand just puts forth a probability-based framework to consider the seismic demand of TCBSBFs.

5.3 Application of the spectral model in seismic design

A three-storey TCBSBF layout is shown in Fig. 13. Under the MCE (Sa=0.5g), the TCBSBF is designed to exhibit damage-control behaviour. The sections of beams, columns and braces are selected properly. The fundamental natural period of the structure is 0.668s. Then the pushover analysis is conducted. From the pushover analysis, we have the post-yield stiffness ratio α = 0.3 and the threshold ductility μ = 3.2. The value of (lnγ)ave and (lnγ)s.dev could be computed using Eq. 3 and 4. Given the structural seismic reliability is 50%, the energy factor γ = 0.941 calculated by Eq. 5. Substituting the data obtained above into Eq. 6, we have the damage-control index D = 0.9 < 1. Therefore, the design of the structure is satisfied.

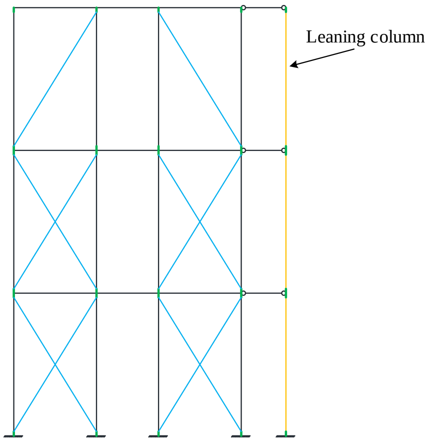

Fig. 13 – Structural layout of TCBSBF

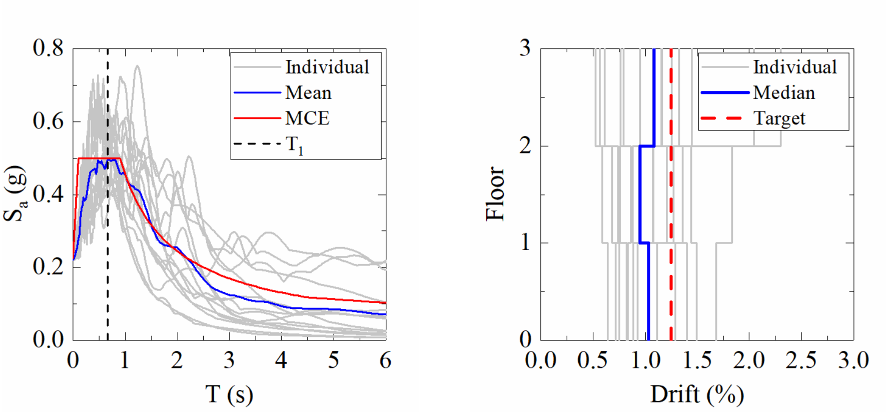

(a) (b)

Fig. 14 – Response history analysis: (a) Pseudo-acceleration response spectra (b) Peak story drift.

In order to validate the structural seismic performance under MCE, the nonlinear response history analyses are conducted. The pseudo-acceleration spectra of scaled records are given in Fig. 14(a). From Fig. 14(b), the median story drift of all the results is below the target story drift threshold. Thus, the seismic performance of the structure is achieved.

6. Conclusions

The seismic demand of the tension-only concentrically braced steel beam-through frames (TCBSBFs) in damage-control stage is quantified using the energy factor in the present study. A pulse-like near-fault ground motion database has been compiled including 320 earthquake records. A parametric study of single-degree-of-freedom (SDOF) systems representing damage-control TCBSBFs is carried out considering the post-yield stiffness ratio (α), the ductility (μ) and the damping ratio (ζ) under the ground motion database. On the basis of the obtained data, the energy factor of TCBSBFs under pulse-like near-fault motions is studied in a statistic way. The probabilistic lognormal model for the energy factor of TCBSBFs is established. The following conclusions can be drawn from the current study:

1. An increasing post-yield stiffness ratio (α) leads to a decreasing energy factor (γ) in the short and moderate period regions, while the tendency is reversed for the long period region. In contrast, a larger ductility (μ) leads to a higher γ in the short and moderate period regions, whereas the tendency is also reversed for the long period region. For the effect of the damping ratio (ζ), a larger ζ leads to an increasing of γ while the reversed tendency can be observed when both α and μ are extremely high. The influence of α and μ on γ is more obvious in the short and moderate period regions than in the long period region. Besides, when α is larger, μ has limited influence on the γ in the long period region.

2. As for the dispersion of the energy factor (γ), it is related to the vibration period (T) of the structure. Specifically, the dispersion of γ is higher in the short and moderate period regions than that in the long period region. The dispersion of γ can be reduced by enhancing α or decreasing μ. Besides, the dispersion of γ is more sensitive to μ, that is, it is more efficient to decrease target μ to reduce the dispersion of γ.

3. The distribution for energy factors (γ) of TCBSBFs obtained from the parametric study generally exhibits a positive skewness. The mode of skewness is related to the structural period under each pair of α and μ. Besides, a smaller α and a larger μ would result in a more evident skewness except for in the extremely short period region. In general, the lognormal distribution could well describe the distribution of the energy factor (γ).

4. For the easy application in practical design and evaluation procedures, two essential parameters, i.e. $(\ln\gamma)_{ave}$ and $(\ln\gamma)_{s.dev}$ in the lognormal distribution model of the energy factor (γ), are fitted by common and concise elementary formulas.

It is worth pointing out that the research findings are based on SDOF analogy in the current study. Hence, the findings should be applied to low-to-medium TCBSBFs governed by the fundamental vibration mode.

7. Acknowledgements

The financial supports from the National Natural Science Foundation of China (Grant No. 51778459 and 51820105013) are gratefully acknowledged. Funding support received from the State Key Laboratory of Disaster Reduction in Civil Engineering, Tongji University (Project No. SLDRCE19-B-05) for the study is also gratefully acknowledged.

8. References

[1] Wang W, Zhou Q, Chen Y, Tong L, Chan T-M (2013): Experimental and numerical investigation on full-scale tension-only concentrically braced steel beam-through frames. *Journal of Constructional Steel Research*, **80** 369-385.

[2] Chen Y, Wang W, Chen Y (2018): Full-scale shake table tests of the tension-only concentrically braced steel beam-through frame. *Journal of Constructional Steel Research*, **148** 611-626.

[3] Filiatrault A, Tremblay R (1998): Design of tension-only concentrically braced steel frames for seismic induced impact loading. *Engineering Structures*, **20** (12), 1087-1096.

[4] Tremblay R, Filiatrault A (1996): Seismic impact loading in inelastic tension-only concentrically braced steel frames: myth or reality? *Earthquake Engineering & Structural Dynamics*, **25** (12), 1373-1389.

[5] Wang W, Du X, Zhang Y, Chen Y (2017): Experimental Investigation of Beam-Through Steel Frames with Self-Centering Modular Panels. *Journal of Structural Engineering*, **143** (5),

[6] Leelataviwat S, Goel S C, Stojadinović B (2002): Energy-based seismic design of structures using yield mechanism and target drift. *Journal of Structural Engineering*, **128** (8), 1046-1054.

[7] Banihashemi M R, Mirzagoltabar A, Tavakoli H (2015): Development of the performance based plastic design for steel moment resistant frame. *International Journal of Steel Structures*, **15** (1), 51-62.

[8] Wongpakdee N, Leelataviwat S, Goel S C, Liao W-C (2014): Performance-based design and collapse evaluation of buckling restrained knee braced truss moment frames. *Engineering Structures*, **60** 23-31.

[9] Goel S C, Liao W C, Reza Bayat M, Chao S H (2010): Performance-based plastic design (PBPD) method for earthquake-resistant structures: an overview. *The structural design of tall and special buildings*, **19** (1-2), 115-137.

[10] Sahoo D R, Chao S-H (2010): Performance-based plastic design method for buckling-restrained braced frames. *Engineering Structures*, **32** (9), 2950-2958.

[11] Kharmale SB, Ghosh S (2013): Performance-based plastic design of steel plate shear walls. *Journal of Constructional Steel Research*, **90** 85-97.

[12] Heidari A, Gharehbaghi S (2015): Seismic performance improvement of special truss moment frames using damage and energy concepts. *Earthquake Engineering & Structural Dynamics*, **44** (7), 1055-1073.

[13] Xiang Y, Luo YF, Huang QL, Zhu ZC (2018): Probabilistic inelastic seismic demand spectra for large-span planar steel structures subjected to vertical ground motions. *Engineering Structures*, **174** 646-662.

[14] Housner G W (1956): Limit design of structures to resist earthquakes. *Proc. of 1st WCEE*.

[15] Newmark N M, Hall W J (1982): Earthquake spectra and design. *Earthquake Eng. Research Institute*, Berkeley, CA.

[16] Leelataviwat S, Goel S C, Stojadinovic B i (1999): Toward performance-based seismic design of structures. *Earthquake Spectra*, **15** (3), 435-461.

[17] Ke K, Ke S, Chuan G (2015): The energy factor of systems considering multiple yielding stages during ground motions. *Soil Dynamics and Earthquake Engineering*, **71** 42-48.

[18] Fang C, Zhong Q, Wang W, Hu S, Qiu C (2018): Peak and residual responses of steel moment-resisting and braced frames under pulse-like near-fault earthquakes. *Engineering Structures*, **177** 579-597.

[19] Hatzigeorgiou G D (2010): Ductility demand spectra for multiple near- and far-fault earthquakes. *Soil Dynamics and Earthquake Engineering*, **30** (4), 170-183.

[20] Dabaghi M (2014): Stochastic modeling and simulation of near-fault ground motions for performance-based earthquake engineering, UC Berkeley.

